Top and gluons at lepton colliders

Cosmin Macesanu and Lynne H. Orr
University of Rochester, Rochester, NY 14627-0171

In this talk we present results of an exact calculation of gluon radiation in top production and decay at lepton colliders, including all spin correlations and interferences. We compare properties of gluons radiated in the production and decay stages and investigate the sensitivity of interference effects to the top decay width.

I. INTRODUCTION

Future high energy lepton colliders — e^+e^- and $\mu^+\mu^-$ will provide relatively clean environments in which to study top quark physics. Although top production cross sections are likely to be lower at these machines than at hadron colliders, the color-singlet initial states and the fact that the laboratory and hard process center of mass frames coincide give lepton machines some advantages. Strong interactions effects such as those due to gluon radiation must still be considered, of course. Jets from radiated gluons can masquerade as quark jets, which can complicate top event identification and mass reconstruction from its decay products, especially for the hadronic decay modes.

In this talk we consider gluon radiation in top quark production and decay ([1]; see also [2]). We consider only collision energies well above the top pair production threshold, so that our results do not depend on whether the initial state consists of electrons or muons. We focus on distributions of radiated gluons and their effects on top mass reconstruction.

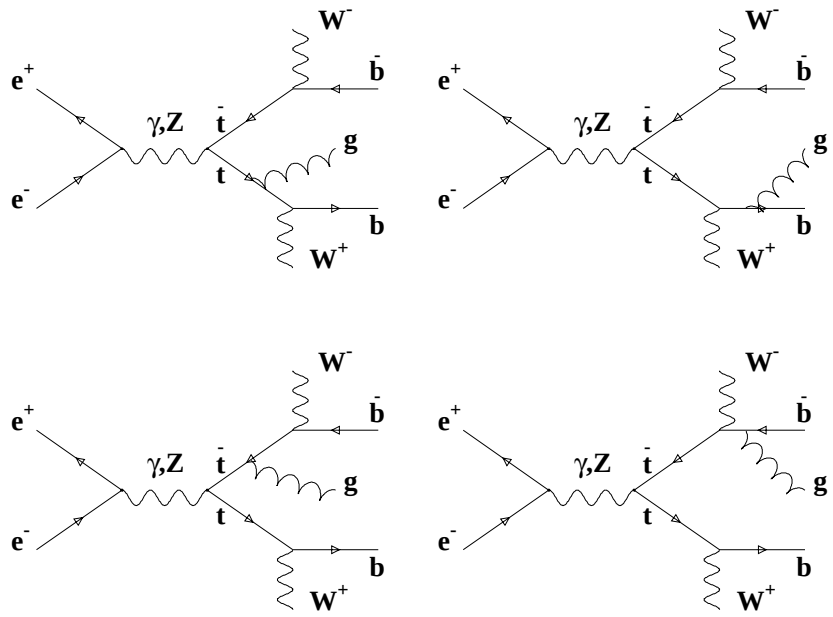

FIG. 1. Feynman diagrams for gluon emission in top production and decay at lepton colliders.

In top events at lepton colliders, there are no gluons radiated from the color-singlet initial state. Final-state gluon emission can occur in both the production and decay processes, with gluons emittied from the top or bottom quarks (or antiquarks), as shown in Figure 1. Emission from the top quark contributes to both production- and decay-stage radiation, depending on when the top quark goes on shell. Emission from the b quarks contributes to decay-stage radiation only.

II. MONTE CARLO CALCULATION

The results presented here are from a Monte Carlo calculation of real gluon emission in top quark production and decay:

$$e^+e^- \to \gamma^*, Z^* \to t\bar{t}(g) \to bW^+\bar{b}W^-g \; . \tag{1}$$

We compute the exact matrix elements for the diagrams shown in Figure 1 with all spin correlations and the bottom mass included. We keep the finite top width , $_t$ in the top quark propagator and include all interferences between diagrams, and we use exact kinematics in all parts of the calculation. We do not include radiation from the decays of the W boson; this amounts to assuming either that the W decays are leptonic or that radiative hadronic W decays can be identified and separated out, for example by invariant mass cuts.

We are particularly interested in the reconstruction of the top quark momentum (and hence its mass) from its decay products. In an experiment this allows us both to identify top events and to measure the top quark's mass. A complication arises when gluon radiation is present, because the emitted gluon may or may not be a top decay product. If it is, then we should include it in top reconstruction, i.e. we have $m_t^2 = p_{Wbg}^2$ for decay-stage radiation. But if the gluon is part of top production, then we have $m_t^2 = p_{Wbg}^2$. It is therefore desirable to be able to identify and distinguish production-stage gluons from those emitted in the decays.

Although this distinction cannot be made absolutely in an experiment, the various contributions can be separated in the calculation. As noted above, gluon emission from the top quark (or antiquark) contributes to both the production and decay stages. These can be separated in the calculation as follows. For definiteness, we consider gluon emission from the top quark, shown in the bottom left diagram in Figure 1. The matrix element contains propagators for the top quark both before and after it radiates the gluon. The matrix element therefore contains the factors

$$ME \propto \left(\frac{1}{p_{Wbg}^2 - m_t^2 + im_t, \; _t} \right) \left(\frac{1}{p_{Wb}^2 - m_t^2 + im_t, \; _t} \right) \; . \tag{2}$$

The right-hand side can be rewritten as

$$\frac{1}{2p_{Wb} * p_{Wbg}} \left(\frac{1}{p_{Wb}^2 - m_t^2 + im_t, \; _t} - \frac{1}{p_{Wbg}^2 - m_t^2 + im_t, \; _t} \right) \; . \tag{3}$$

This separates the production and decay contributions to the matrix element because the two terms in parentheses peak respectively at $p_{Wb}^2 = m_t^2$ (production emission) and $p_{Wbg}^2 = m_t^2$ (decay emission). The cross section in turn contains separate production and decay contributions. It also contains interference terms, which in principle confound the separation but in practice are quite small.

In fact the interference terms are interesting in their own right, although not for top reconstruction. In particular, the interference between production- and decay-stage radiation can be sensitive to the top quark width , $_t$, which is about 1.5 GeV in the Standard Model. [3] The interference between the two propagators shown above can be thought of as giving rise to two overlapping Breit-Wigner resonances. The peaks are separated roughly by the gluon energy, and each curve has width , $_t$. Therefore when the gluon energy becomes comparable to the top width, the two Breit-Wigners overlap and interference can be substantial. In constrast, if the gluon energy is much larger than , $_t$, overlap and hence interference is negligible. Hence the amount of interference serves as a measure of the top width. We will explore this more below.

III. NUMERICAL RESULTS

A. Overall Gluon Properties

We begin our numerical results with the relative contributions of production- and decay-stage radiation to the total cross section. Figure 2 shows the fraction of the total cross section due to production stage emission, in events with an

extra gluon. The solid line is for center-of-mass energy 1 TeV, and the dashed line is for 500 GeV. Both curves fall off as the minimum gluon energy increases; this reflects the decrease in phase space for emitted gluons. The production fraction is higher at a 1 TeV collision energy than at 500 GeV — again this reflects phase space — but decay-stage radiation always dominates for both cases.

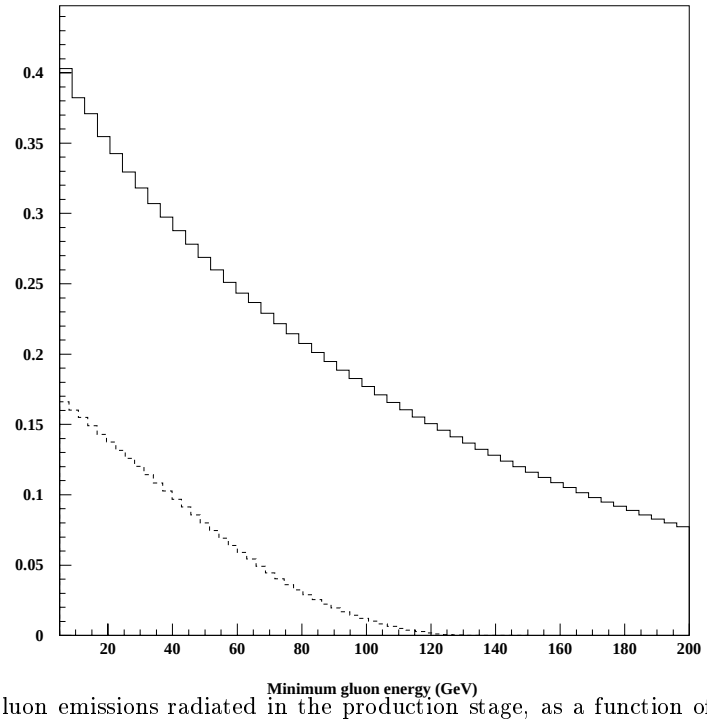

FIG. 2. The fraction of gluon emissions radiated in the production stage, as a function of minimu gluon energy, for center-of-mass energy 1 TeV (solid line) and 500 GeV (dashed line).

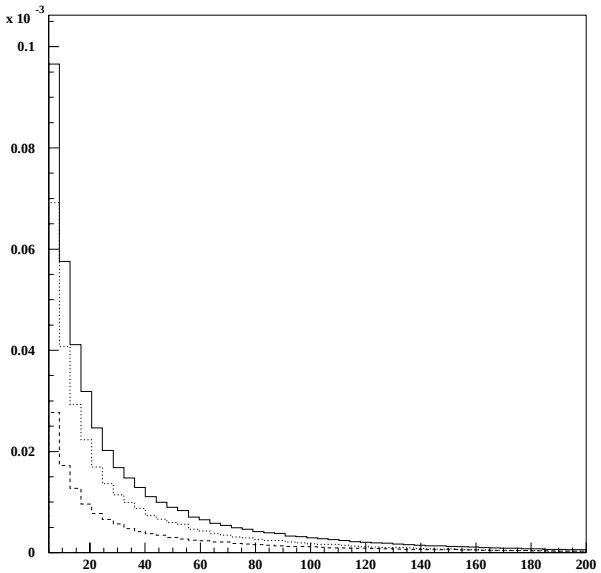

FIG. 3. The spectrum of radiated gluons as a function of gluon energy in GeV. Dashed histogram: production-stage radiation. Dotted histogram: decay-stage radiation. Solid histogram: total.

Figure 3 shows the total gluon energy spectrum for an intermediate collision energy of 750 GeV along with its decomposition into production (dashed histogram) and decay (dotted histogram) contributions. Again we see that deca-stage radiation dominates. Otherwise the spectra are not very different; both exhibit the rise at low energies due to the infrared singularity characteristic of gluon emission, and both fall off at high energies as phase space runs out.

B. Mass Reconstruction

We now turn to the question of mass reconstruction. Figure 4 shows top invariant mass distributions with and without the extra gluon included. In both cases there is a clear peak at the correct value of m_t. In the left-hand plot, where the gluon is not included in the reconstruction, we see a low-side tail due to events where the gluon was radiated in the decay. Similarly, in the right-hand plot we see a high-side tail due to events where the gluon was radiated in association with production, and was included when it should not have been.

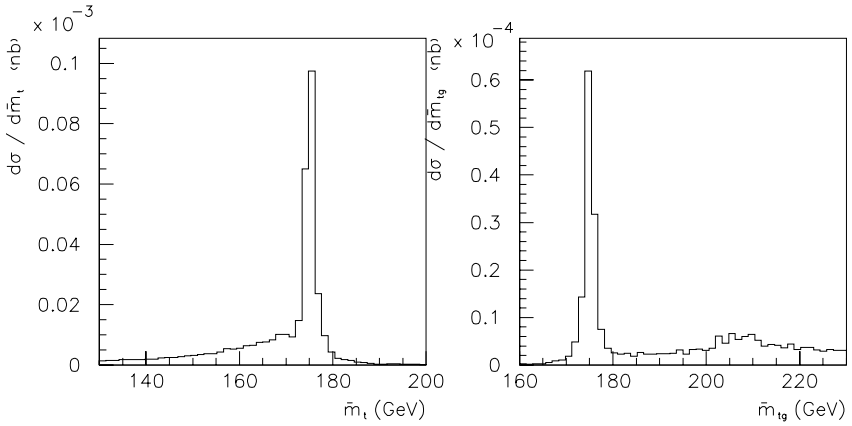

FIG. 4. The top invariant mass spectrum without (left) and with (right) the gluon momentum included, for center-of-mass energy 600 GeV.

The narrowness of the peaks and the length of the tails in Figure 4 suggests that an invariant mass cut would be useful to separate the two types of events. We can do even better by considering cuts on the angle between the gluon and the b quarks. This works because although there is no collinear singularity for radiation from massive quarks, the distribution of gluons radiated from b quarks peaks close to the b direction. Such gluons are emitted in decays. The dotted histogram in Figure 5 shows the top mass distribution that results from using proximity of the gluon to the b quarks to assign the gluon.

Of course an importnat reason the cuts are so effective is that we work at the parton level. The experimentalists do not have that luxury, and, as one would expect, hadronization and detector effects are likely to cloud the picture. The solid histogram in Figure 5 shows the mass distribution after including energy smearing; the solid curve is a Gaussian fit. The spread in the measured energies is parametrized by Gaussians with widths $\sigma = 0.4\sqrt{E}$ for quarks and gluon, and $\sigma = 0.15\sqrt{E}$ for the W's. We see that the central value does not shift, but the distribution is significantly wider.

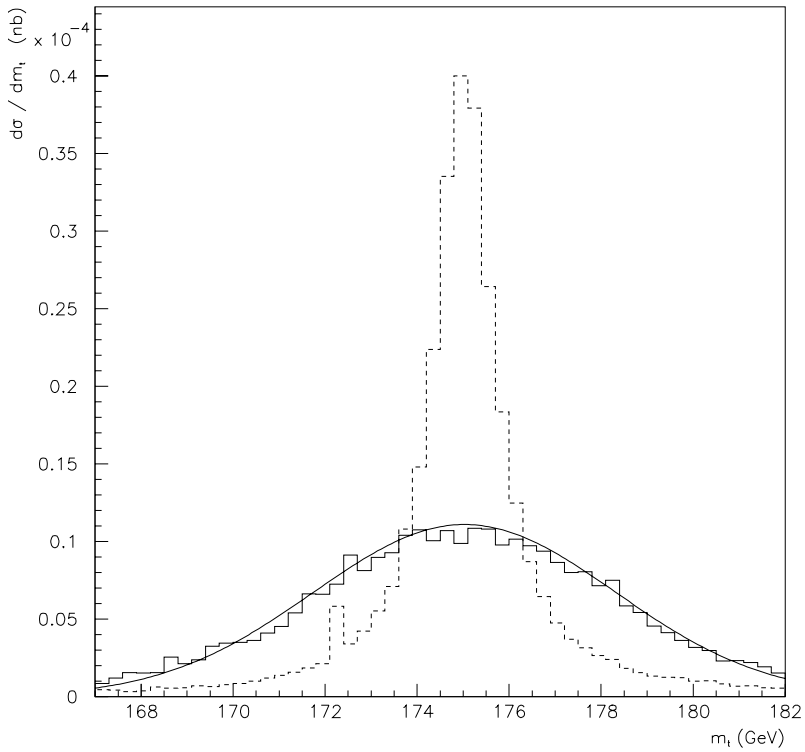

FIG. 5. The top invariant mass spectrum with b-gluon angle selection criteria (dotted histogram), for center-of-mass energy 600 GeV and minimum gluon energy 10 GeV. The solid curve and histogram show the effects of energy smearing.

C. Interference and Sensitivity to Γ_t

Finally, we return to the subject of interference. As mentioned above, the interference between the production- and decay-stage radiation is sensitive to the total width of the top quark Γ_t. However because the interference is in general small, we need to find regions of phase space where it is enhanced. This question was considered in Ref. [3] in the soft gluon approximation, where it was found that the interference was enhanced when there was a large angular separation between the t quarks and their daughter b's.

Here we examine whether the result of [3] survives the exact calculation. Figure 6 shows that it does. There we plot the distribution in the angle between the emitted gluon and the top quark for gluon energies between 5 and 10 GeV and with $\cos\theta_{tb} < 0.9$. The center-of-mass energy is 750 GeV. The histograms show the decomposition into the various contributions. The negative solid histogram is the production-decay interference, and we see that not only is it substantial, it is also destructive. That means that the interference serves to suppress the cross section. If the top width is increased, the interference is larger, further suppressing the cross section. this is illustrated in Figure 7, which shows the cross section for different values of the top width. Although the sensitivity does not suggest a precision measurement, it is worth noting that the top width is difficult to measure by any means, and it is the total width that appears here. At the very least such a measurement would serve as a consistency check.

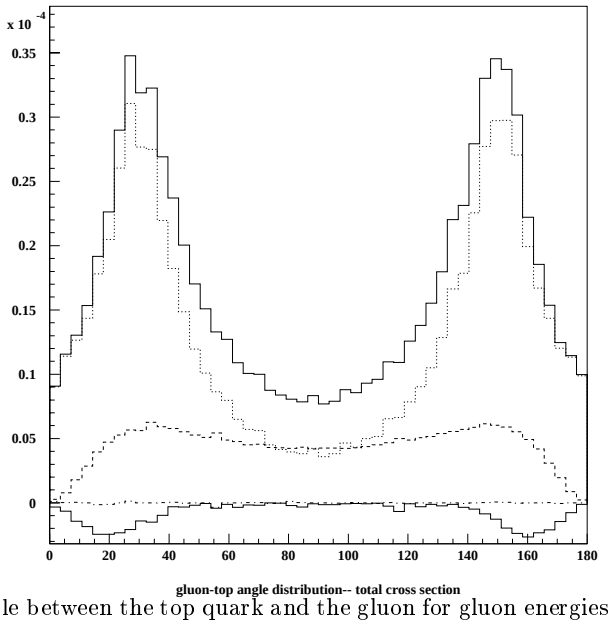

FIG. 6. The distribution in angle between the top quark and the gluon for gluon energies from 5 to 10 GeV, $\cos\theta_{tb} < 0.9$, and 750 GeV collision energy. The upper solid histogram is the total and the other histograms represent the individual contributions: dotted: decay; dashed: production; dot-dashed: decay-decay interference; solid: production-decay interference.

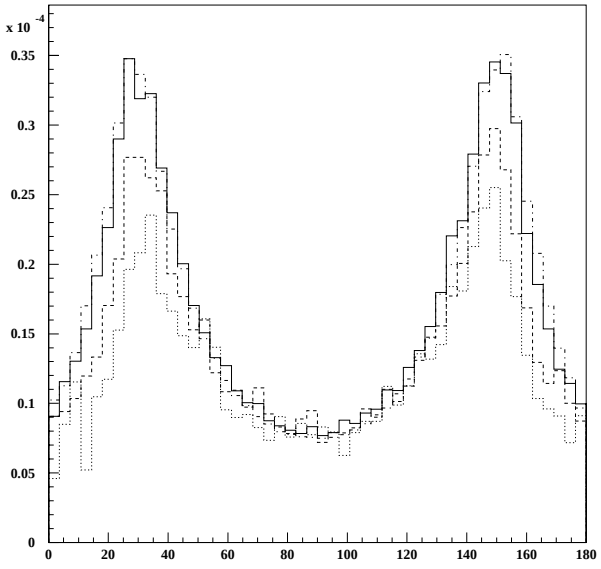

FIG. 7. The distribution in angle between the top quark and the gluon for gluon energies from 5 to 10 GeV, $\cos\theta_{tb} < 0.9$, and 750 GeV collision energy. The histograms correspond to different values of the top width , $_t$: dot-dashed: 0.1 GeV; solid: 1.5 GeV (SM); dotted: 5. GeV; dotted: 20 GeV.

IV. CONCLUSION

In summary, we have presented preliminary results from an exact parton-level calculation of real gluon radiation in top production and decay at lepton colliders, with the b quark mass and finite top width, as well as all spin correlations

and interferences included. We have indicated some of the issues associated with this gluon radiation in top mass reconstruction and top width sensitivity in the gluon distribution. Further work is in progress.

This work was supported in part by the U.S. Department of Energy and the National Science Foundation.

---

[1] C. Macesanu and L.H. Orr, in preparation.
[2] C.R. Schmidt, Phys. Rev. **D54** 3250 (1996).
[3] V. Khoze, L.H. Orr and W.J. Stirling, Nucl. Phys. **B378** 413 (1992).